CANARD INFLUENCE ON THE BOUNDARY LAYER OF A FORWARD SWEPT WING

G. Lombardi
Assistant Professor, Department of Aerospace Engineering, University of Pisa, Italy

M. Morelli, D. Waller
Research Engineers, Medium Speed Wind Tunnel, CSIR, Pretoria, South Africa

Abstract

The effect of a lifting canard on the transition from laminar to turbulent flow in the boundary layer of a forward swept wing is experimentally analysed. The study is based on surface flow visualization, carried out on the upper surface of the wing by means of the liquid crystals technique. The results show that with a lifting canard the transition in the wing boundary layer occurs in three different modes, depending on the spanwise position. This behaviour is probably related to different phenomena, viz. the turbulence in the canard wake, particularly inside the tip vortex, and the important increase in the spanwise pressure gradient and cross flow, which could lead to a different type of instability. Over the whole wing span the transition in the canard configuration occurs further upstream than on the isolated wing, for the same wing lift. It is evident that the significant upstream displacement in the boundary layer transition, caused by the lifting canard, gives rise to a significant increase in the wing friction drag, with a reduction in the aerodynamic efficiency.

Nomenclature

AR	=	aspect ratio
b	=	span (m)
c	=	local chord (m)
C_l	=	sectional lift coefficient
C_L	=	wing lift coefficient
c_{mean}	=	mean geometric chord (m)
L	=	stagger, horizontal distance between the points at x/c=0.3 of the wing and the canard, at the root section (m)
Re	=	Reynolds number
T	=	gap, vertical distance between the points at x/c=0.3 of the wing and the canard, at the root section (m)
U_∞	=	free stream velocity (m/sec)
x	=	distance from wing section leading-edge (m)
y	=	spanwise distance measured from wing root (m)
α	=	angle of attack (deg)
γ	=	decalage, angle defined by the directions of the wing and canard chords, Fig. 1 (deg)
Λ	=	sweep angle at 1/4 of the chord (deg)
λ	=	taper ratio
ζ	=	grey level non-dimensional parameter

subscripts

c	=	canard
w	=	wing

Introduction

Aircraft with fore horizontal stabilizing surfaces (canards) have been developed in recent years, both in the general aviation and in the high performance fields. To obtain real advantages, a thorough knowledge of the flow behaviour over these configurations is necessary. Some of the capabilities offered by these configurations were extensively analysed in a cooperation between the Department of Aerospace Engineering of the University of Pisa and the Aerotek Division of the Council for Scientifical and Industrial Research of Pretoria (CSIR). In particular, global force measurements,[1] and accurate pressure measurements on the wing surfaces[2,3] were carried out. Information on the basic canard-wing flow in both the subsonic and transonic regimes was obtained from the results. From the above analysis it was clear that the canard effects are significantly dependent on its dimensions and relative position with respect to the wing. As discussed in Ref. 4, a canard can be used to increase the aerodynamic efficiency of the configuration, as regards both to the stall behaviour and the shaping of span lift distribution to produce a lower value of the lift dependent drag.

By utilising canards positioned above the wing (+T), very small variations in the aerodynamic characteristics of the wing can be observed; on the contrary, low or coplanar canard positions greatly affect the pressure field on the

wing, and can also be used to increase the aerodynamic efficiency of the configuration. For this purpose a wing with a flow type adequately supported by the canard interference should be used, as, for instance, a forward-swept wing. Indeed, coupling the canard surface with a forward swept wing seems to give strong advantages from the aerodynamic point of view, as can be seen from the analysis carried out in Ref. 3 and, more in detail, in Ref. 5. However, it is evident that no definitive conclusions on the aerodynamic behaviour of a configuration can be achieved without an analysis of its influence on the boundary layer conditions. This analysis is necessary to predict the stall characteristics and the friction drag contribution to the total drag of the airplane. In particular, the friction drag, which is highly dependent on boundary layer state, represents a significant part of the total drag; from this point of view it is interesting to note that the theoretical and experimental analyses presented by Redeker and Wicmann[6] showed that the fore sweep gives the advantage of a more stable laminar boundary layer.

In this paper the effects of a lifting canard surface on the transition from laminar to turbulent flow in the boundary layer of a forward swept wing are analysed.

Fundamentals on boundary layer transition

For the purpose of our analysis, it is important to identify the general mechanisms that enhance transition from laminar to turbulent flow in a boundary-layer. A clear basic description is reported, for instance, in the review of Saric and Reed.[7] With the receptivity process,[8] disturbances in the free stream enter the boundary layer as steady and/or unsteady fluctuations of the basic state. The initial growth of these disturbances can be described as a linear process; this growth is weak and occurs over a viscous time scale. As the amplitude grows, three-dimensional and non-linear interactions occur in the form of secondary instabilities. Disturbance growth is very rapid in this case, occurring in a convective time scale, and breakdown to turbulence occurs. Typically, this type of flow is susceptible to four types of instabilities. The leading edge instability is associated either with a basic instability of the attachment-line flow or with turbulent disturbances that propagate along the leading edge. The streamwise instability is associated with the flow chordwise velocity component and is quite similar to processes in 2-D flows, where Tollmien-Schlichting waves generally develop. Centrifugal instability occurs in the shear flow over a concave surface and appear in the form of Gortler vortices. The cross-flow instability occurs when both strong pressure gradients and significant velocity components in the cross direction are present.

It is clear that a wide range of parameters can influence the type and evolution of the disturbances in the boundary layer; these parameters include wing sweep, airfoil shape, pressure gradient, weather conditions, surface roughness height and distribution.

For the specific problem of a swept wing, the transition is quite a complex phenomenon. Although transition involves unsteady modes, the role of stationary cross-flow vortices can be important. Crouch[9] has shown, with the receptivity theory, that roughness elements on the wing surface can generate stationary wave instabilities with initial amplitudes much larger than that of the travelling waves, thus dominating the transition process. In effect, prior to transition, both stationary and travelling streamwise vortices have been experimentally observed, for instance by Arnal et al.,[10] Bippes and Nitschke-Kowsky,[11] and Dagenhart et al.[12] These streamwise vortices are cross-flow instabilities spawned from inflections in the mean velocity profile, and they are prevalent in regions of favourable pressure gradients (i.e., near the leading edge), where Tollmien-Schlichting waves are suppressed. Near the pressure gradient crossover point, travelling waves can become unstable, and potential interactions from these unstable waves with cross-flow vortices that are already present may cause the transition from laminar to turbulent flow.

More recently, the importance of the cross-flow instability for swept wings was confirmed by direct numerical simulation. Joslin and Streett[13] and Joslin[14] computed the spatial evolution of stationary cross-flow vortices in a laminar boundary layer on a swept wing. They found that the vortex disturbances first enter a chordwise region that can be described as linear growth, then the individual disturbances coalesce downstream, and either superimpose linearly or interact non linearly with adjacent waves. Finally, the cross-flow vortices enter a region that contains strong non-linear interactions. In this later stage, the low velocity fluid near the wing surface is lifted out into the boundary layer and rolled over the high-speed fluid in the direction of the positive spanwise velocity component, with highly inflectional chordwise and spanwise velocity profiles, and a rapid growth of secondary instabilities, which lead to the catastrophic breakdown to turbulence. Liu and Domaradzki,[15] by means of direct numerical simulation of the evolution of a three dimensional Gortler flow, also showed that the spanwise inflectional profile and the associated shear velocity gradient play an important role in the transition process. Furthermore, stationary cross flow waves on a swept airfoil have been experimentally investigated by Rebert et al.,[16] within a low-disturbance environment; they showed that, also with a very polished surface, stationary cross flow was still dominating the transition process. Finally, Ahmed et al.[17] observed the presence of cross flow vortices in flight conditions as well.

For high aspect ratio wings, travelling waves may became unstable along the attachment-line and may cause transition at the outboard or inboard portion of the wings (depending on the cross-flow direction). It is important to note that travelling waves are observed in tunnels rich in unsteady free stream disturbances, whereas stationary waves dominate in a low turbulence environment, as

Stability of Mach number with time	$\sigma_{Mt} \leq 0.0014$			
Stability of stagnation pressure with time	$\sigma_{P_0} \leq 0.0012$ KPa			
Stability of stagnation temperature with time	$\sigma_{T_0} \leq 2$ °K			
Humidity level dewpoint	2° below tunnel static temperature			
Spatial variation of Mach number	$\sigma_M \leq 0.002$	(subsonic);	$\sigma_M \leq 0.004$	(supersonic)
Spatial variation of flow angularity	$\sigma_\mu \leq 0.15°$	(subsonic);	$\sigma_\mu \leq 0.30°$	(supersonic)
Acoustic pressure coefficient fluctuation	$\Delta c_p \leq 0.01$			
Acoustic fluctuation frequency content	$[n\ F(n)]^{1/2} \leq 0.007$			
Turbulence level	$\sigma_u/U_\infty \leq 0.001$ (low Mach);		$\sigma_u/U_\infty \leq 0.002$	(high Mach)

(σ = root mean square)

Tab. 1 - Main flow characteristics in the wind tunnel test section

shown, for instance, by Muller and Bippes,[18] and Bippes et al.[19] In any case, Meyer and Kleiser[20] show that the transition process on a swept wing depends strongly on the chosen initial disturbances. Therefore, it is evident that significant differences in the boundary layer state could appear when flight conditions and wind tunnel experiments are compared. In experimental conditions a control of the initial disturbances field is difficult because freestream turbulence, wind tunnel noise, tunnel-wall interference, and imperfections on the surfaces are always present in various degrees.

Furthermore, it is necessary to note that not only transition but also separation of the boundary layer could be affected by the different instability modes present in the experiments; in fact, the separation lines are highly dependent on the boundary layer conditions (laminar or turbulent). As a consequence, when wind tunnel results are used for a flight condition prediction, the difference in Reynolds number might not be the more important effect, and care must be taken when wind tunnel evaluation of transition and separation lines are considered.

From the above described mechanisms of the transition to turbulence in a swept wing boundary layer, it is clear that the extension to canard configurations of the behaviour observed for isolated wings is not immediate; indeed, transition depends on several parameters that could be modified by the canard surface as, for instance, the turbulence level of the flow over the wing.

Experimental set-up

The wind tunnel

The tests were carried out in the Medium Speed Wind Tunnel of the CSIR facilities, in South Africa. This is a closed circuit variable density transonic wind-tunnel. Its operational speed ranges from M=0.25 to M=1.5 with pressure varying from 20 kPa to 250 kPa; Reynolds number can be changed by modifying the pressure. The test section has a 1.5m x 1.5m square cross section, 4.5m in length, enclosed in a plenum. All four walls are equally longitudinally slotted for a total porosity of 5%. The behaviour of the wind tunnel as regards blockage is very satisfactory, as can be seen from the results of the dedicated tests described in Ref. 21. The main flow characteristics in the test section are summarised in Tab. 1, derived from the complete calibration of the wind tunnel, presented in Ref. 22.

The configuration analysed

The adopted geometric conventions are shown in Fig.1; on the basis of the results described in Refs. 1 and 3, the relative position between wing and canard was chosen to be characterised by a fixed stagger, as defined in Fig.1, equal to 2.26 mean geometric chords of the wing.

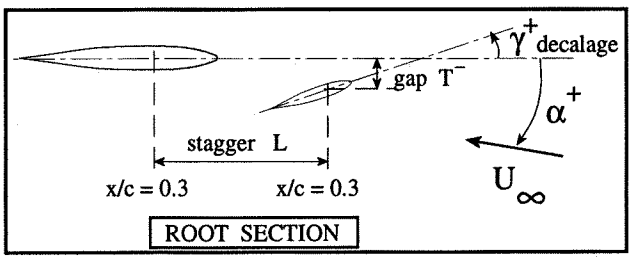

Fig. 1 - The adopted conventions

A configuration with a low positioned canard seems to be less interesting for practical applications, because it is characterised by a strong modification of the wing aerodynamic characteristics,[3,5] and the control of the flow may become difficult. For instance, in Ref. 23 it was shown that the canard tip vortex can split in two well defined vortices at the wing leading edge. Therefore, a coplanar configuration (T/L=0) was used in this phase of the research. Furthermore, a decalage angle γ of 2.5° was fixed, since in typical configurations the canard is positioned at higher angle of attack than the wing.

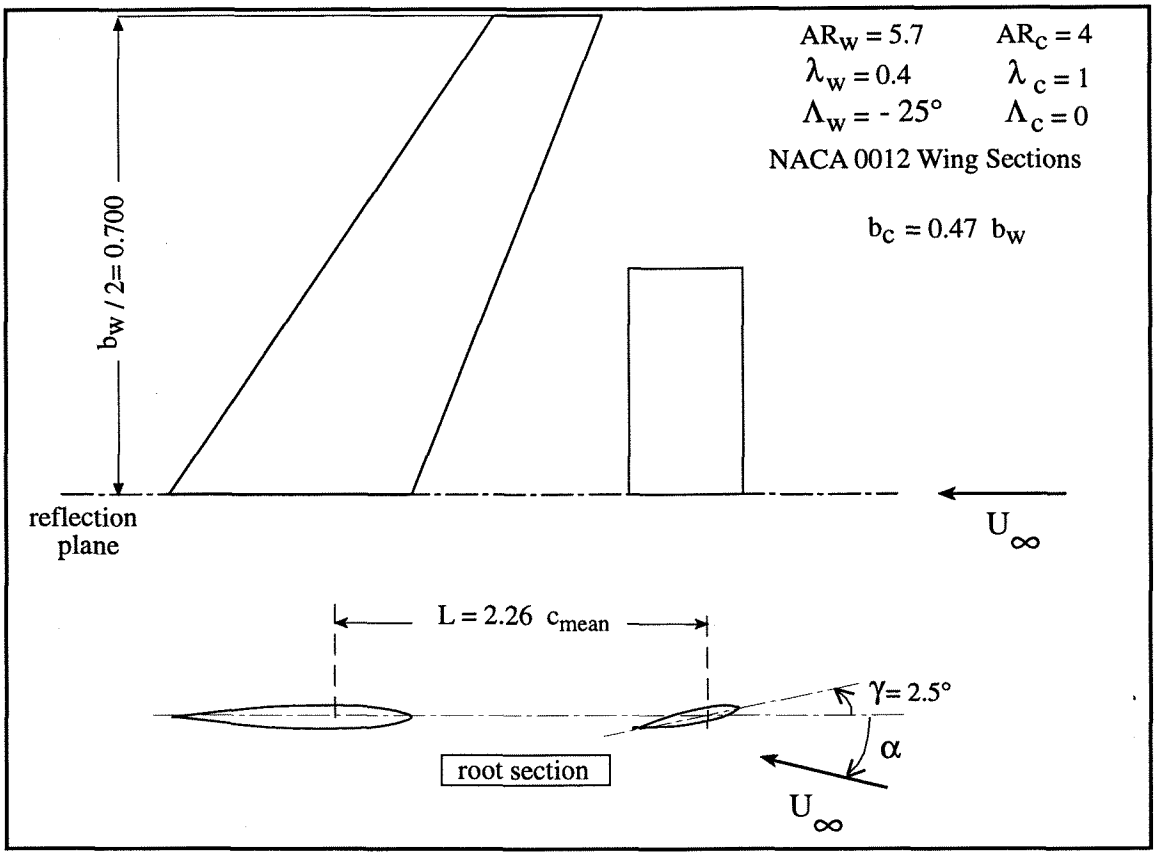

Fig. 2 - Definition of the analysed configuration

The forward swept wing model described in Ref. 2 was used; it is a wing with zero twist and dihedral angles, aspect ratio 5.7, taper ratio 0.4, sweep angle, at 1/4 of the chord, Λ=-25° and a NACA 0012 wing section. The canard model[3] is a unswept rectangular lifting surface with zero twist and dihedral angles, aspect ratio 4, NACA 0012 wing section and a span equal to 0.47 of the wing span. The analysed configuration is shown in Fig.2. Because of the symmetry of the problem a side wall support with a splitter-plate was used to reduce the interference between the wing and the wall boundary layers.

The models were machined from a 7075 aluminium alloy plate using Numerical Control Technology; on the wing model, pressure ports were fitted to obtain a total of 320 measurement points, with 10 span stations and 32 chord points, as defined in Ref. 2. The formulation of the error analysis, both for positioning and for pressure measurements, has been described in Ref. 24, where the dimensional control carried out on the shape of both canard and wing models and on the position of the orifices is also reported. The model surface is polished to a 1.5 μm r.m.s. finish.

The force coefficients on the wing were evaluated by means of numerical integration of the pressure distributions, as indicated in Ref. 2. The global lift coefficient is non-dimensionalised with the free-stream dynamic pressure and the wing planform area. The sectional lift coefficients along the span are non-dimensionalised with the free-stream dynamic pressure and the local chord.

In the present paper, the experiments carried out at a Mach number of 0.3 are considered, with two Reynolds numbers, of approximately 1.9×10^6 and 2.8×10^6 based on the wing mean aerodynamic chord. The turbulence level in these conditions is lower than 0.001, as can be seen from Tab 1. The analysis is carried out on the upper surface of the wing, where the effects of the interaction with the canard wake are more important.

Flow visualization technique

The flow visualization technique is based on liquid crystal paint. The advantages of this technique are well specified, for example, in Refs. 25-27, where an introduction to its use is also reported.

The main feature of liquid crystal materials is the reversible deformation of their internal structure when they are subjected to temperature and/or tangential stress variations; optical phenomena of selective reflection are connected with such a deformation. Therefore, by utilizing

liquid crystals that are non-dependent on temperature, for fixed lighting and viewing angles, the scattered colour of the light reflected by the crystals depends on the local shear stress; by analysing the changes in the colour, details on boundary layer transition and flow separation are obtained. A more complete description of the method is reported in Ref. 28, where several examples of the effects produced by the liquid crystal painting are shown.

The brightness of the reflected colours is related to the lighting characteristics. It is not possible to have general rules, and for each test the best lighting technique must be found. Several combinations of lighting technique and viewing points were investigated in Ref. 28, and the results showed that a "diffused" light source and a viewing point "normal" to the surface are preferable. Therefore, the set-up described in Fig 3 was chosen.

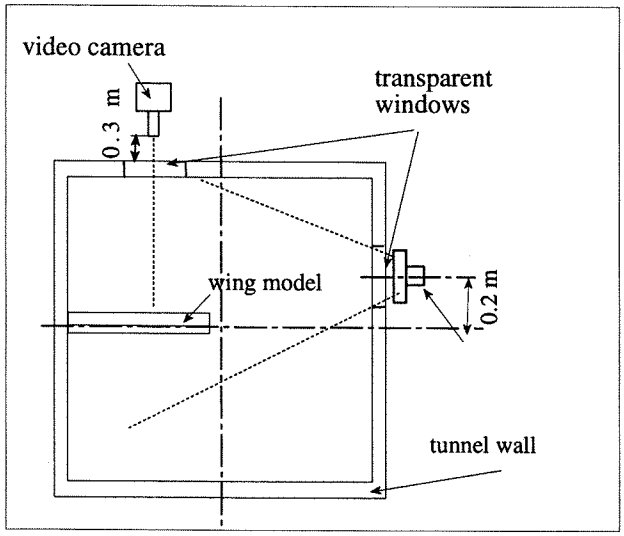

Fig. 3 - Layout of lighting and viewing - rear view (not in scale)

The images of the model surface, acquired by means of a video camera, were recorded on a video tape and, successively, transferred to an image processor. By means of the image processing a passage from a coloured image analysis to a grey-level analysis is carried out,[28] the white corresponding to the lower limit of the liquid crystal response (red) and the black to the higher limit (violet). With this passage the information for each pixel in which the surface is subdivided by the video camera resolution, is reduced to only one (the grey level). With a 8 bit grey-level resolution, the value 0 corresponds to the black and the value 255 to the white; it is useful to use a non-dimensional parameter, defined as:

$$\zeta = (255 - \text{value}) / 255$$

It is clear that the conversion from colour to a grey scale is not unique, and that the operation must be guided by the operator to ensure that the grey image captures the important features of the colour image to be analysed, without adding or blanking features.

With the above definition, the parameter ζ ranges from 0 (stress level less than the minimum observable by the specific liquid crystal) to 1 (stress level higher than the maximum observable by the specific liquid crystal).

Naturally, the information given by the parameter ζ can not be assumed as absolute, but only qualitative; the "true" information does not concern the numerical value itself, but the change in this value, that indicates a change in the local tangential stress, and, therefore, a modification in the boundary layer condition.

As an example, the isolines of the parameter ζ are shown in Fig. 4, for the isolated wing at $\alpha=0°$ and $Re=2.8x10^6$. By analysing this figure it is possible to determine the transition line, corresponding to the maximum gradient.

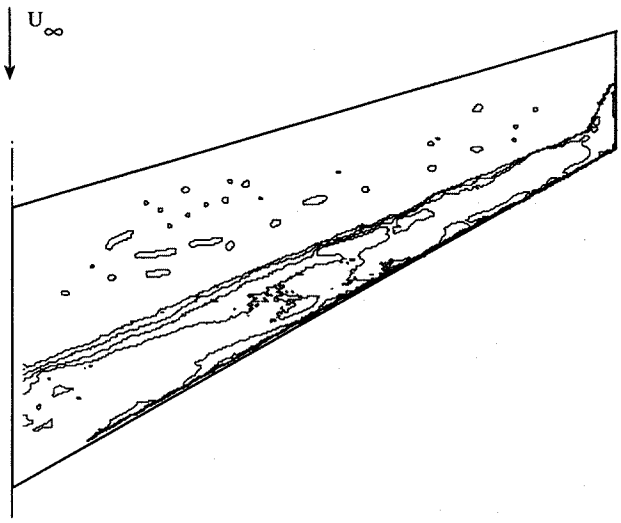

Fig. 4 -Isolines of the parameter ζ ; $\alpha=0°$, $Re=2.8x10^6$

In the following discussion, for clarity, only the transition lines determined from the gradient of the parameter ζ will be reported.

Analysis of the results

Fig. 5 shows the C_L-α curves of the wing for the canard-on and canard-off configurations.

The behaviour is almost linear up to about $C_L=0.8$, when zones of separated flow appear on the wing for both configurations.[3,5]

The presence of a lifting canard produces significant downwash in the inboard zone and upwash in the outboard zone of the wing. For the specific configuration this results in a reduction of the wing lift at a given angle of attack, while the slope of the C_L-α curve remains approximately the same.

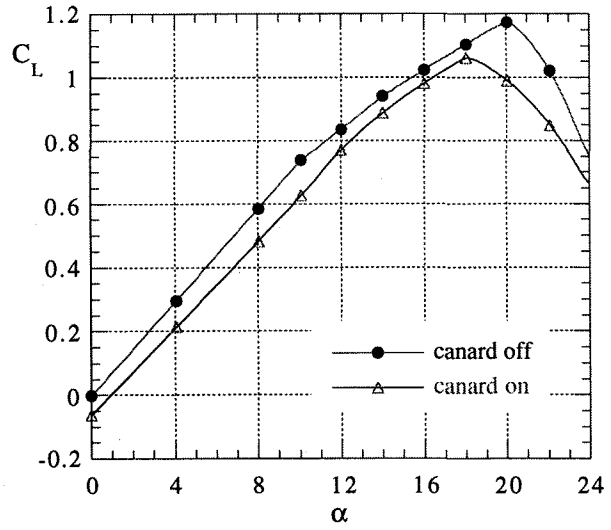

Fig. 5 - Wing global lift coefficient versus angle of attack

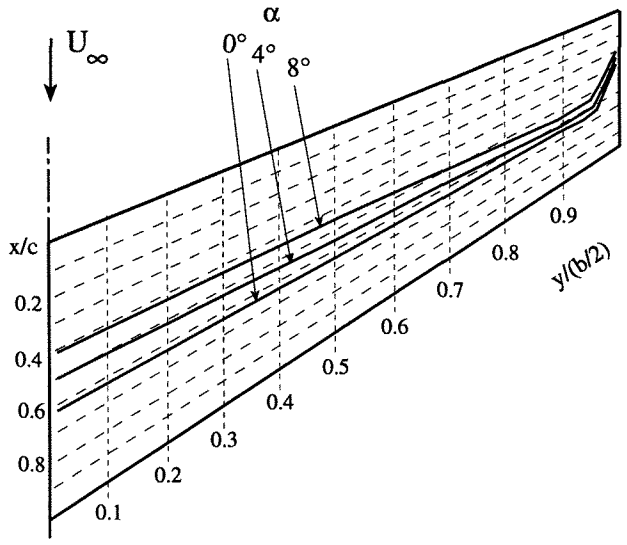

Fig. 6 - Transition lines for the isolated wing; Re=2.8x10^6

The isolate wing shows a transition line from laminar to turbulent boundary layer that is practically straight along the span (see Fig. 6), except than in a small zone close to the wing tip, characterized by a significant up-stream displacement of the transition line. This displacement, present at all the angles of attack, seems to be related to the turbulence produced by the tip vortex, which originates along the tip in a position between 0.3 to 0.5 chords downstream of the leading edge.[29] At low angles of attack the transition occurs at almost constant x/c and, therefore, it occurs at the root at a larger distance downstream of the leading edge. Increasing the angle of attack, as expected, transition moves up-stream. It is interesting to note that this displacement is higher at the root than at the tip; indeed, at the root transition moves from about x/c=0.63 at α=0° to about x/c=0.41 at α=8°, while close to the tip (y/(b/2)=0.9) the transition moves from about x/c=0.67 at α=0° to about x/c=0.58 at α=8°. As a consequence, at α=8° the transition occurs at a practically constant distance from the leading edge. This behaviour is probably related to the appearance of a cross flow, in the inboard direction for a forward swept wing, which provokes an instability of the travelling waves; on the contrary, at α=0°, the cross flow is practically absent for the present wing, and the streamwise instability of the Tollmien-Schlichting waves is probably the cause of transition.

In Fig. 7 the transition lines at α=0° for different Reynolds number are shown. As expected, an up-stream displacement is present when Reynolds number increases, and the characteristics of transition lines at about constant x/c is maintained.

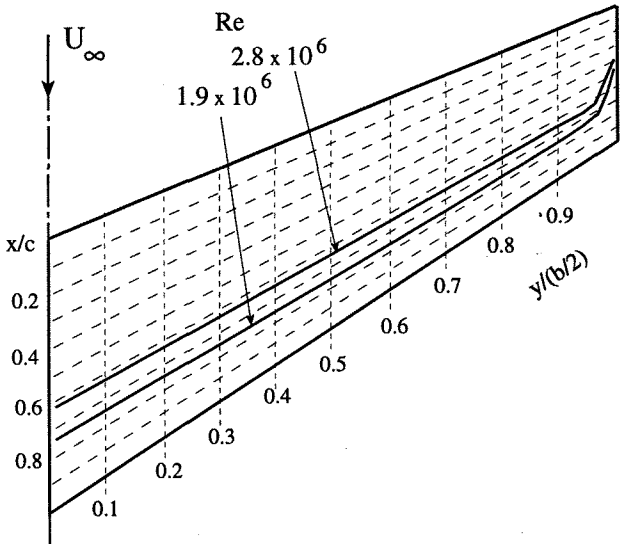

Fig. 7 - Transition lines for the isolated wing - Effect of the Reynolds number; α=0°

Fig. 8 shows the transition lines for the configurations with and without canard, for the condition of no global lift acting on the wing, C_L=0. As can be seen, the behaviour of the two cases is completely different. In the canard configuration the transition is anticipated along all the span, and three different zones can be identified: an inner zone, a middle zone and an outer zone.

The middle zone has an extension of about ten per cent of the semi-span, and is characterised by a completely turbulent boundary layer. This zone is interacting directly with the canard tip vortex, which produces, in this zone, a "free-stream" characterized by a very high turbulence level.

To analyse the inner and outer zones it is necessary to take into account that, as can be seen from Fig. 9, in the configuration with the lifting canard the spanwise lift distribution on the wing is strongly modified. Indeed, in the canard configuration the spanwise pressure gradients and the cross flow become more important, and probably lead to a cross-flow instability. The appearance of this

type of instability, enhanced by the higher amplitude of the perturbation caused by the turbulent flow in the middle zone, causes the flow transition in the boundary layer to occur sooner, both in the inner and in the outer zones. Moreover, in the outer zone the higher local angles of attack (see again Fig. 9) enhance the fore transition displacement, while in the inner zone the interaction with the canard wake increases the turbulence level of the stream flowing over the wing, with a consequent upstream displacement of the transition. As a conclusion, the transition is displaced upstream over the entire wing span.

Fig. 10 shows the transition lines for the configurations with and without canard, at a wing lift coefficient C_L=0.58, corresponding to an angle of attack of about 8° for the isolated wing and about 9.5° for the canard configuration. Qualitatively, the effect of the canard remains that described previously for the C_L=0 case. The transition is again characterized by three different zones. As previously, in the middle zone the flow is completely turbulent; an inboard displacement of this zone is observed, consequent to the inner displacement of the canard tip vortex when the angle of attack increases.[30]

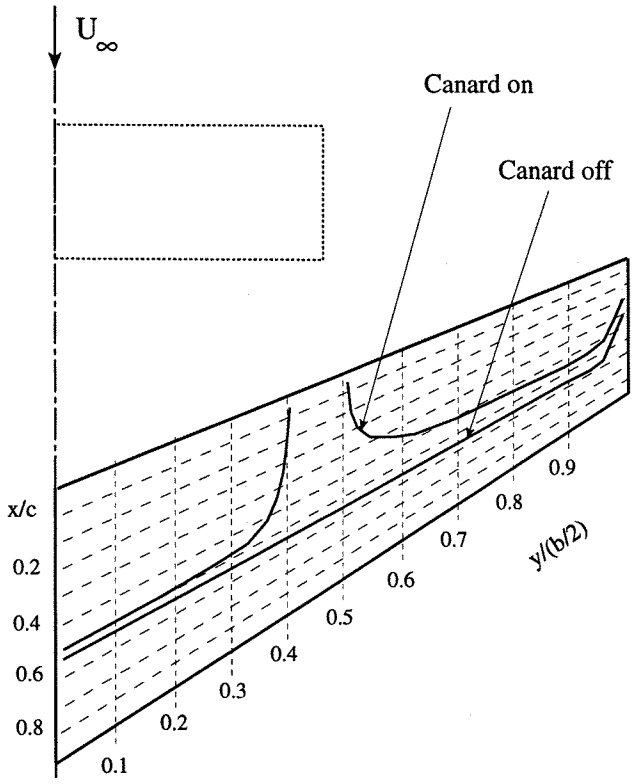

Fig. 8 - Canard effect on the transition lines; C_L=0

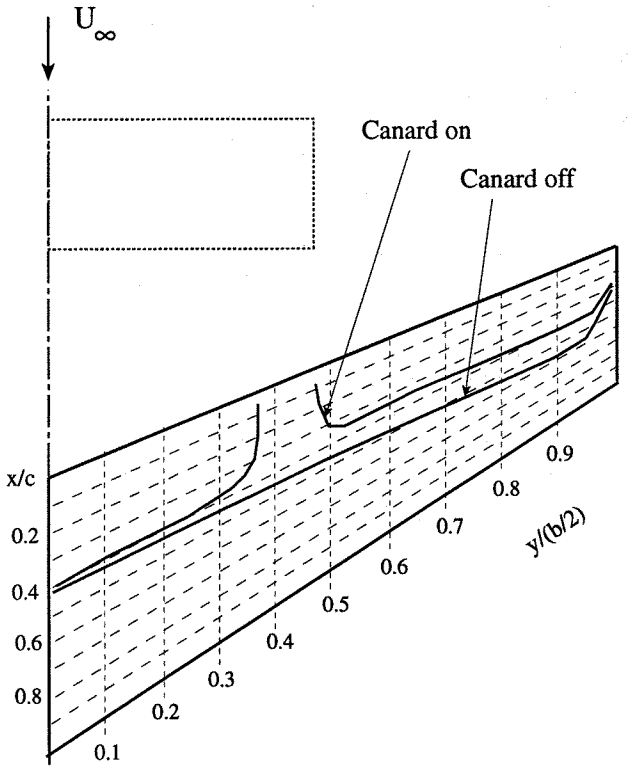

Fig. 10 - Transition lines; C_L=0.58

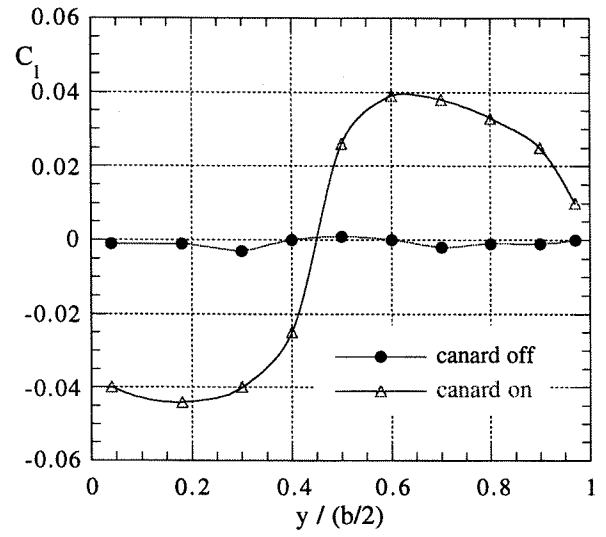

Fig. 9 - Spanwise lift coefficients; C_L=0

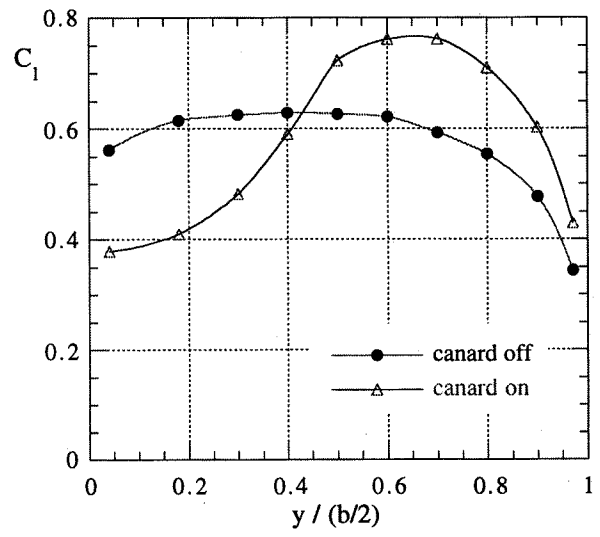

Fig. 11 - Spanwise lift coefficients; C_L=0.58

The spanwise extension of this zone remains practically the same, but it is not possible to assume this as a general trend. In fact, two different effects on the extension of this zone can be expected when the angle of attack increases: the increase in the dimension of the canard tip vortex, tends to broaden it, while the higher distance between the canard tip vortex and the wing surface has a narrowing effect. In the specific case a cancellation between these two opposite effects probably occurs.

In the inner zone the transition moves upstream, even though, in the analysed condition, the local angles of attack in this zone are significantly lower than for the isolated wing, as can be seen by analysing the spanwise lift distributions shown in Fig. 11.

This is probably related to the perturbation incoming from the canard wake and from the turbulent middle zone, and also to the high spanwise pressure gradient and important cross flow, directed in the inboard direction.

In the outer zone the transition occurs more upstream with respect to the isolated wing condition, probably because of the significantly higher local angles of attack (see again Fig. 11). In any case, it is possible to observe that the transition occurs slightly more upstream than in the inner zone, and this can be a confirmation of the importance of the cross-flow type instability in the inner zone of the wing. This type of instability becomes particularly significant in the canard configuration, leading to a remarkable upstream displacement of the boundary layer transition.

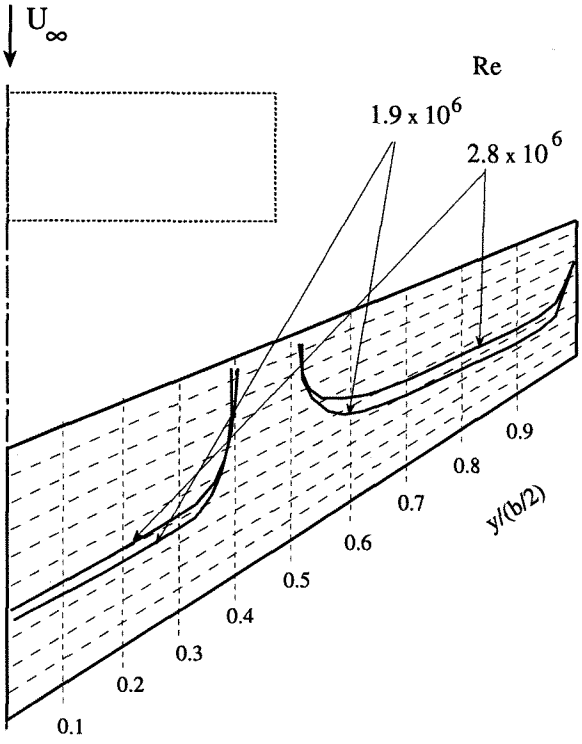

Fig. 12 - Transition lines for the isolated wing - Effect of the Reynolds number; C_L=0°

The effect of the Reynolds number is shown in Fig. 12 for the C_L=0 case. As expected, an upstream transition occurs when the Reynolds number increases. The middle zone of completely turbulent flow is slightly larger at lower Reynolds number, in agreement with the higher canard tip vortex dimension in this condition.

Conclusions

The effect of a lifting canard on the transition from laminar to turbulent flow in a forward swept wing boundary layer was analysed by means of surface flow visualisations.

The results showed that when a lifting canard is used, the transition on the wing occurs differently in three zones, depending on the spanwise position. In all the zones, on the upper surface of the wing, the transition moves upstream with respect to the case of the isolated wing with the same lift. Two main effects are probably present: the turbulence in the canard wake, particularly in the tip vortex, which gives a completely turbulent flow over the part of the wing directly interacting with it, and an important increase of the spanwise pressure gradients and of the cross flow. This could change the instability from a streamwise type to a cross flow type. In a forward swept wing this instability mode produces more important effects close to the wing root, and this is enhanced by the lifting canard, that produces high spanwise pressure gradients and cross flow velocities (in the inboard direction) in the inner part of the wing.

The extension of these results to flight conditions is not immediate. Indeed, while in the zone of completely turbulent flow, in direct interference with the canard tip vortex, the phenomenon is clearly non-dependent on the specific freestream characteristics, in the remaining zones the different characteristics between real and wind tunnel conditions could change the instability modes and, consequently, the transition lines. This aspect can be important also when numerical evaluations are carried out. In fact the usual numerical methods are based on formulations requiring semi-empirical parameters, and it could be necessary to modify their setting to correctly take into account the canard effects.

However, it is evident that the important upstream displacement in the boundary layer transition, caused by the lifting canard, produces a significant increase in the wing friction drag. This disadvantage is more important at low Reynolds number conditions, characterized by a large extension of the laminar flow.

Finally, it is important to observe that the described behaviour could be inconsistent with a drag reduction method based on the laminar flow control, if criteria developed for classical configurations are followed. On the other hand, it is possible that, with a laminar flow control specifically developed for canard configuration, the disadvantage of friction drag increase might be less important.

References

[1] Buresti, G. and Lombardi, G., "Indagine Sperimentale Sull'Interferenza Ala-Canard," *L'Aerotecnica, Missili e Spazio,* Vol. 67, no. 1-4, 1988, pp. 47-57.

[2] Lombardi, G., "Experimental study on the Aerodynamic Effects of a Forward Sweep Angle," *Journal of Aircraft*, Vol. 30, No. 5, Sep.-Oct. 1993.

[3] Lombardi, G. and Morelli, M., "Pressure Measurements On A Forward Swept Wing-Canard Configuration," *Journal of Aircraft*, Vol. 31, No. 2, Mar.-Apr. 1994.

[4] Lombardi, G. and Vicini, A., "Induced Drag Prediction for Wing-Tail and Canard Configurations through Numerical Optimization," *The Aeronautical Journal* ,Vol. 98, No. 976, Jun.-Jul. 1994.

[5] Lombardi, G. and Morelli, M., "Aerodynamic Experimental Analysis of Canard Configurations with a Forward Swept Wing," in La Ricerca e Ricercatori della Facoltà di Ingegneria, ETS Ed., Feb. 1995, Pisa.

[6] Redeker, G. and Wichmann, G., "Forward Sweep-A Favorable Concept for a Laminar Flow Wing," *Journal of Aircraft*, Vol. 28, Feb. 1991, pp. 97-103.

[7] Saric, W. S. and Reed, H. L., "Stability and Transition of Three-Dimensional Boundary Layer," in AGARD CP 438, Oct. 1988.

[8] Morkovin, M. V., "Instability, Transition to Turbulence and Predictability," in AGARDograph 236, 1977.

[9] Crouch, J. D., "Receptivity of Three-Dimensional Boundary Layers," AIAA Paper 93-0074, 1993.

[10] Arnal, D., Coustols, E. and Jullien, J. C., "Experimental and Theoretical Study of Transition Phenomena on an Infinite Swept Wing," *La Recherche Aerospace*, 1984-2, Mar.-Apr. 1984, pp. 275-290.

[11] Bippes, H. and Nitschke-Kowsky, P., "Experimental Study of Instabilities Modes in a Three-Dimensional Boundary Layer," AIAA Paper 87-1336, 1987.

[12] Dagenhart, J. R., Saric, W. S., Mousseux, M. C. and Stack, J. P., "Crossflow-vortex Instability and Transition on a 45-degree Swept Wing," AIAA Paper 89-1892, 1989.

[13] Joslin, D. and Streett, C. L., "The Role of Stationary Cross-Flow Vortices in Boundary-Layer Transition on Swept Wings," *Physic of Fluid A*, Vol. 6, 1994, pp. 3442-3453.

[14] Joslin, D, "Evolution of Stationary Crossflow Vortices in Boundary-Layer on Swept Wings," *AIAA Journal*, Vol. 33, Jul. 1995, pp. 1279-1285.

[15] Liu, W. and Domaradzki, J. A., "Direct Numerical Simulation of Transition to Turbulence in Gortler Flow," *Journal of Fluid Mechanics*, Vol. 246, 1993, pp. 267-299.

[16] Reibert, M. S., Saric, W. S., Carrillo, R. B.. and Chapman, K. L., "Experiments in Nonlinear Saturation of Stationary Crossflow Vortices in a Swept-Wing Boundary Layer," AIAA Paper 96-0184, 1996.

[17] Ahmed, A., Wentz, W. H. and Nyenhuis, R., "In Flight Boundary-Layer Boundary Layer Transition Measurements on a Swept Wings," *Journal of Aircraft*, Vol. 26, Nov. 1989, pp. 979-985.

[18] Muller, B. and Bippes, H., "Experimental Study of Instabilities Modes in a Three-Dimensional Boundary Layer," in AGARD CP 438, 1988.

[19] Bippes, H., Muller, B. and Wagner, M., "Measurements and Stability Calculations of the Disturbances Growth in an Unstable Three-Dimensional Boundary Layer," *Physic of Fluid A*, Vol. 3, 1991, pp. 2371-2377.

[20] Meyer, F. and Kleiser, L., "Numerical Investigation of Transition in 3D Boundary Layers," in AGARD CP 438, 1988.

[21] Lombardi, G. and Morelli, M., "Analysis of Some Interference Effects in a Transonic Wind Tunnel", *Journal of Aircraft*, Vol. 32, no. 3, May-June 1995, pp. 501-509.

[22] Hurlin, R.S. and Davis, M.W., "Preliminary Calibration Results for the CSIR Medium Speed Wind Tunnel", DAST Report 90-320, Nov. 1990.

[23] Lombardi, G., "Canard tip Vortex Splitting in a Canard-Wing Configuration: Experimental Observations," *Journal of Aircraft*, Vol. 32, no. 4, July-Aug. 1995, pp. 875-877.

[24] Buresti, G., Lombardi, G. and Morelli, M., "Pressure Measurements on Different Canard-Wing Configurations in Subsonic Compressible Flow," Atti del Dipartimento di Ingegneria Aerospaziale, ADIA 91-4, Sept. 1991.

[25] Holmes B.J., Gall P.D., Croom C.C., Manuel G.S. and Kelliher W.C., "A New Method for Laminar Boundary-Layer Transition Visualization in Flight-Color changes in Liquid-Crystals Coatings," NASA TM-87666, 1986.

[26] Parmar D.S., "A Novel Technique for Response Function Determination of Shear Sensitive Cholesteric Liquid Crystals for Boundary Layer Investigation," Rev. Sci. Instrum., Vol. 62, No. 6, June 1991.

[27] Smith S.C., "Use of Shear-Sensitive Liquid Crystals for Surface Flow Visualization," *Journal of Aircraft*, Vol. 29, No. 2, March-April 1992.

[28] Lombardi, G., Morelli, M. and Waller, D., "Flow Visualization with Shear Sensitive Liquid Crystal - Some Examples and Problems," Proceedings of the 7th Flow Visualization Symposium, Sept. 1995, pp. 526-531.

[29] Lombardi, G. and Cannizzo, F., "High Aspect Ratio Wings: Tip Vortex Structure And its Numerical Implications," AIAA Paper 96-1961, June 1996.

[30] Lombardi, G., "Vorticity Structure in the Near-Field of a Wing Tip Vortex ," submitted for pubblication to the AIAA Journal, Mar. 1996.